MITSUBISHI ELECTRIC RESEARCH LABORATORIES
http://www.merl.com

Wideband Diversity in Multipath Channels with Nonuniform Power Delay Profiles

Win, M.; Chrisikos, G.

TR2003-68 August 2003

Abstract

The focus of this paper is to derive the symbol error probability (SEP) of a Rake receiver with a limited number of fingers that track the strongest multipath components in a frequency-selective Rayleigh fading channel. We develop an analytical framework that allows the computation of the SEP for nonuniform power delay profiles (PDPs) and spreading bandwidth. By transforming the physical Rake receiver with correlated ordered paths into the domain of a virtual Rake receiver with conditionally independent virtual paths, analytical expressions for the SEP are derived in terms of the spreading bandwidth, the channel profile, and the number of combined paths. We show how our analytical results can be used to predict the performance of various Rake architectures in environments with nonuniform PDPs using for example, the channel models defined for the next generation wireless standards. Furthermore, we validate our methodology by comparison to data obtained from channel measurements, showing good agreement with our analytically derived results.

Publication History:

1. First printing, TR-2003-68, August 2003

Wideband Diversity in Multipath Channels with Nonuniform Power Delay Profiles

Moe Z. Win[†], *Senior Member, IEEE*, George Chrisikos, *Senior Member, IEEE*, and Andreas F. Molisch, *Senior Member, IEEE*

Corresponding Address:

Laboratory for Information and Decision Systems (LIDS)

Massachusetts Institute of Technology

Cambridge, MA 02139 USA

Tel.: (732)-687-8113

e-mail: moewin@mit.edu

Moe Z. Win was with the Wireless Systems Research Department, AT&T Labs - Research Middletown, NJ 07748-4801, USA. He is now with the Laboratory for Information and Decision Systems (LIDS), Massachusetts Institute of Technology, Cambridge, MA 02139 USA (e-mail: moewin@mit.edu).

George Chrisikos can be reached at (e-mail: gchrisikos@alumni.usc.edu).

Andreas F. Molisch was with the Wireless Systems Research Department, AT&T Labs - Research, Middletown, NJ, USA. He is now with Mitsubishi Electric Research Laboratory, Cambridge, MA, USA and the Department of Electroscience, Lund University, Lund, Sweden (e-mail: Andreas.Molisch@ieee.org).

[†]Corresponding author.

Abstract

The focus of this paper is to derive the symbol error probability (SEP) of a Rake receiver with a limited number of fingers that track the strongest multipath components in a frequency-selective Rayleigh fading channel. We develop an analytical framework that allows the computation of the SEP for nonuniform power delay profiles (PDPs) and spreading bandwidth. By transforming the physical Rake receiver with correlated ordered paths into the domain of a "virtual Rake" receiver with conditionally independent virtual paths, analytical expressions for the SEP are derived in terms of the spreading bandwidth, the channel profile, and the number of combined paths. We show how our analytical results can be used to predict the performance of various Rake architectures in environments with nonuniform PDPs using for example, the channel models defined for the next generation wireless standards. Furthermore, we validate our methodology by comparison to data obtained from channel measurements, showing good agreement with our analytically derived results.

I. INTRODUCTION

A key benefit of wide bandwidth systems is that the large transmission bandwidth allows resolution of the multipath components with different delays encountered in the wireless channel [1], [2]. The resolved multipaths can then be combined using Rake receivers to exploit the multipath (delay) diversity [3], [4].

There has been a significant deployment of spread spectrum (SS) multiple access techniques in wireless communication systems in recent years, and they are widely used for third generation wireless access [5]–[10]. In principle, the Rake receiver in these wide bandwidth systems can resolve and combine all multipath components with delay spacing greater than the chip time T_{c} (approximately equal to the inverse of the spreading bandwidth). For a dense multipath channel with a fixed maximum excess delay T_{d}, the number of resolvable multipath components N_{r} increases with the spreading bandwidth. However, hardware implementations impose limitations on the utilization of the number of multipath components; i.e., practical Rake receivers can often process only a subset of the available multipath components [11]. This leads to the structure

of the selective Rake (SRake) receiver [12]–[16]. The SRake receiver is a multipath combining system that selects the L best paths (a subset of the available resolved multipath components) and then combines the selected subset using maximal-ratio combining (MRC) [3]. This technique provides improved performance over L-path combining while reducing the complexity over the all-Rake (ARake) receiver that combines all the N_{r} resolved multipath components.

The symbol error probability (SEP) of such Rake receivers in the aforementioned setting is thus of great practical as well as theoretical interest. In particular, next generation wireless standards define channel models with various power delay profiles (PDPs) [17], [18].[1] Hence in this paper, we consider the SEP performance of the SRake receiver operating in channels with various PDPs. We consider PDPs with nonuniform magnitude, unequal delay spacing and arbitrary phase. In a previous paper [16], we presented an approach suitable for a uniform PDP. This case was analyzed using a "virtual path" technique, which results in a simple SEP expression for any L and N_{r}. The key idea of the virtual path technique as applied to the constant PDP case is to transform the dependent ordered multipath components into a new set of virtual paths that are independent. We assumed that instantaneous estimation of all possible multipaths is feasible such as with slow fading.

For a nonuniform PDP, we show here that the virtual path technique can also be applied, but the virtual paths are now *conditionally* independent. This results in an analytically tractable derivation of the SEP for a given spreading bandwidth and any number of combined paths in the SRake receiver operating in dense multipath channels with a nonuniform PDP.[2] The SEP is obtained as a linear combination of single integrals with finite limits.

An important tradeoff in receiver design is to quantify the number of fingers that should

[1]The PDP is a characterization of the dispersion of a mulitpath channel in the delay domain. The dispersion of a channel is caused by the scattering encountered in the operational environment and is a dual of the frequency selectivity of the channel.

[2]We first outlined this idea in [19]. An alternative computational method can be found in [20], which uses the so-called "spacing" method and does not utilize the chain rule of conditional expectation that is central to our derivation.

be active in Rake receivers at any one time. We show how the spreading bandwidth, channel profile and the number of combined paths all affect the SEP. As an example of using our derivations with realistic PDP's, we consider the channel model developed by the International Telecommunications Union, known as the ITU-R channel model standard [17]. Finally, we also apply our evaluation method to measurement results. Specifically, the results of a measurement campaign in an urban environment in Germany is evaluated and compared to our method, showing good agreement with our analytical results.

The paper is organized as follows: Sec. II introduces the SRake receiver, and derives the SEP using the "virtual path" technique. We also show how the general expressions can be simplified for the single-path (SP) receiver and ARake receiver. Next, we demonstrate the effect of spreading bandwidth, shape of the PDP, and the number of Rake fingers in Sec. III using ITU-R PDPs for numerical examples. We also compare the results of the measurement campaign to theoretical results in Sec. III. Conclusions are given in Sec. IV.

II. SRake Receiver Performance Analysis

A. The SRake Receiver

The matched filter version of the SRake receiver involves a matched front-end processor (MFEP) followed by a tapped-delay line and a selection combiner. Let γ_i denote the instantaneous SNR of the MFEP output samples. The instantaneous output SNR of the SRake combiner is

$$\gamma_{\text{SRake}} = \sum_{i=1}^{L} \gamma_{[i]} \qquad 1 \leq L \leq N_{\text{r}}\,, \tag{1}$$

where $\gamma_{[i]}$ is the ordered γ_i, i.e., $\gamma_{[1]} > \gamma_{[2]} > \ldots > \gamma_{[N_{\text{r}}]}$, and N_{r} is the number of available multipath components.

We consider a slowly varying wide-sense stationary uncorrelated scattering (WSSUS) channel with frequency selective fading. This channel is modeled as a two-dimensional complex Gaussian

process with zero-mean and nonuniform PDP, which results in a p.d.f. of the instantaneous branch SNR given by

$$f_{\gamma_i}(x) = \begin{cases} \frac{1}{\Gamma_i} e^{-\frac{x}{\Gamma_i}}, & 0 < x < \infty \\ 0, & \text{otherwise}\,. \end{cases} \tag{2}$$

where the mean $\Gamma_i \triangleq \mathbb{E}\{\gamma_i\} = \frac{R_{\rm y}(t_i,t_i)}{R_{\rm n}(t_i,t_i)}$. The correlation functions $R_{\rm y}(t_1,t_2)$ and $R_{\rm n}(t_1,t_2)$ of the MFEP outputs are due respectively to the signal and noise.

Consider a MFEP with equivalent lowpass (ELP) impulse response

$$f_{\rm M}(t) = \begin{cases} s^*(T_{\rm s}-t), & 0 < t < T_{\rm s} \\ 0, & \text{otherwise}\,, \end{cases} \tag{3}$$

where $s(t)$ denotes the ELP transmitted signal having energy $2E_{\rm s}$, and symbol duration $T_{\rm s}$. For a slowly varying WSSUS channel, the correlation function of the MFEP output is presented in [16] as

$$R_{\rm y}(t_1,t_2) = \begin{cases} \displaystyle\int_{-\infty}^{+\infty} P_{\rm h}(0,\tau)\widetilde{R}_{\rm s}^*(t_1-T_{\rm s}-\tau) \\ \quad \times \widetilde{R}_{\rm s}(t_2-T_{\rm s}-\tau)d\tau & \text{for } \ |t_2-t_1| < \frac{2}{B_{\rm s}} \\ \quad 0 & \text{otherwise}\,. \end{cases} \tag{4}$$

where $P_{\rm h}(0;\tau)$ is the PDP, also known as the multipath intensity profile, and

$$\widetilde{R}_{\rm s}(t-T_{\rm s}-\tau) \triangleq \int_0^{+\infty} s(t-\alpha-\tau) f_{\rm M}(\alpha)\, d\alpha\,. \tag{5}$$

In SS parlance, $\widetilde{R}_{\rm s}(\tau)$ is the periodic time auto-correlation function of the baseband spread signature sequence. Similarly, the correlation function of $n_{\rm M}(t)$ is given by

$$\begin{aligned} R_{\rm n}(t_1,t_2) &= \int_0^{+\infty}\int_0^{+\infty} \mathbb{E}\{n^*(t_1-\alpha_1)n(t_2-\alpha_2)\} f_{\rm M}^*(\alpha_1) f_{\rm M}(\alpha_2)\, d\alpha_1 d\alpha_2 \\ &= 2N_0 \widetilde{R}_{\rm s}(t_2-t_1)\,. \end{aligned} \tag{6}$$

In deriving (6) we have used the property that $\mathbb{E}\{n^*(t_1-\alpha_1)n(t_2-\alpha_2)\} = 2N_0\delta_{\rm D}(t_2-t_1+\alpha_1-\alpha_2)$, where $\delta_{\rm D}(\cdot)$ is the Dirac delta function. In this study, the instantaneous SNR of the

MFEP output samples are assumed to be independent. The justification of this assumption can be found in [16].

Let $\mathcal{S}_{N_\mathrm{r}}$ be the set of all permutations of integers $\{1, 2, \ldots, N_\mathrm{r}\}$, and let $\sigma \in \mathcal{S}_{N_\mathrm{r}}$ denote the particular mapping $\sigma : (1, 2, \ldots, N_\mathrm{r}) \rightarrow (\sigma_1, \sigma_2, \ldots, \sigma_{N_\mathrm{r}})$ which permutes the integers $\{1, 2, \ldots, N_\mathrm{r}\}$. Note that the cardinality of $\mathcal{S}_{N_\mathrm{r}}$ is equal to $N_\mathrm{r}!$ where $N_\mathrm{r}! = N_\mathrm{r}(N_\mathrm{r} - 1) \cdots 1$. Denoting $\boldsymbol{\gamma}_{[N_\mathrm{r}]} \triangleq (\gamma_{[1]}, \gamma_{[2]}, \ldots, \gamma_{[N_\mathrm{r}]})$, and letting $(x_{[1]}, x_{[2]}, \ldots, x_{[N_\mathrm{r}]})$ be the associated integration variables, it can be shown that the joint p.d.f. of $\gamma_{[1]}, \gamma_{[2]}, \cdots, \gamma_{[N_\mathrm{r}]}$ is

$$f_{\boldsymbol{\gamma}_{[N_\mathrm{r}]}}\left(\{x_{[i]}\}_{i=1}^{N_\mathrm{r}}\right) \tag{7}$$
$$= \begin{cases} \displaystyle\sum_{\sigma \in \mathcal{S}_{N_\mathrm{r}}} \prod_{k=1}^{N_\mathrm{r}} \frac{e^{-\frac{1}{\Gamma_{\sigma_k}} x_{[k]}}}{\Gamma_{\sigma_k}}, & x_{[1]} > x_{[2]} > \cdots > x_{[N_\mathrm{r}]} > 0 \\ 0, & \text{otherwise}. \end{cases}$$

It is important to note that the $\gamma_{[i]}$'s are no longer independent, even though the underlying γ_i's are independent.

B. Error Probability Analysis in the Virtual Rake Framework

The SEP for an SRake receiver in a multipath fading environment can be obtained by averaging the conditional SEP over the channel ensemble as[3]

$$P_{e,\text{SRake}} = \mathbb{E}_{\gamma_{\text{SRake}}}\left\{\Pr\left\{e \mid \gamma_{\text{SRake}}\right\}\right\}, \tag{8}$$

where $\Pr\left\{e \mid \gamma_{\text{SRake}}\right\}$ is the conditional probability of error, conditioned on the random quantity γ_{SRake}. Using the technique of [25]–[28], and by substituting the expression for γ_{SRake} directly in terms of the physical branch variables given in (1), we can obtain the desired SEP. As an example, the SEP for coherent detection of M-ary phase-shift keying (MPSK) is given (see, for

[3]Strictly speaking, we derive the matched-filter bound (MFB) [21]–[24]. This is an analytical tool that assumes the absence of intersymbol interference. In spread-spectrum systems, this bound can be achieved or approximated with high spreading gain.

example [16], [28], [29]) by

$$P_{e,\text{SRake}} = \frac{1}{\pi}\int_0^{\Theta} \mathbb{E}_{\{\gamma_{[i]}\}}\left\{ e^{-\frac{\delta_{\text{MPSK}}}{\sin^2\theta}\sum_{i=1}^{L}\gamma_{[i]}} \right\}\, d\theta \tag{9}$$

$$= \frac{1}{\pi}\int_0^{\Theta} \int_0^{\infty}\int_0^{x_{[1]}} \cdots \int_0^{x_{[N_\text{r}-1]}} e^{-\frac{\delta_{\text{MPSK}}}{\sin^2\theta}\sum_{i=1}^{L} x_{[i]}} \tag{10}$$

$$\times \quad f_{\boldsymbol{\gamma}_{[N_\text{r}]}}(\{x_{[i]}\}_{i=1}^{N_\text{r}})\, dx_{[N_\text{r}]}\ldots dx_{[2]}dx_{[1]}\, d\theta\,,$$

where $\delta_{\text{MPSK}} = \sin^2(\pi/M)$ and $\Theta = \pi(M-1)/M$.

Since the statistics of the ordered paths are no longer independent, the evaluation of (10) involves N_r-fold nested integrals, which are in general cumbersome and complicated to evaluate. This can be alleviated by transforming the instantaneous SNR's of the ordered multipath components into a new set of virtual path instantaneous SNR's, V_i's, using the following relationship:

$$\gamma_{[k]} = \sum_{n=k}^{N_\text{r}} \left[\frac{1}{n}\sum_{m=1}^{n}\frac{1}{\Gamma_m}\right]^{-1}\frac{1}{n}V_n\,. \tag{11}$$

Denoting $\boldsymbol{V} \triangleq (V_1, V_2, \ldots, V_{N_\text{r}})$, it can be shown that the joint p.d.f. of $V_1, V_2, \ldots, V_{N_\text{r}}$ is given by

$$f_{\boldsymbol{V}}(\{v_n\}_{n=1}^{N_\text{r}}) = \sum_{\sigma\in\mathcal{S}_{N_\text{r}}} \Pr\{\sigma\}\, f_{\boldsymbol{V}\big|_\sigma}(\{v_n\}_{n=1}^{N_\text{r}} \,\big|\, \sigma)\,, \tag{12}$$

where $f_{\boldsymbol{V}\big|_\sigma}(\{v_n\}_{n=1}^{N_\text{r}} \,\big|\, \sigma)$ is the conditional p.d.f. of $\boldsymbol{V}$, conditioned upon the quantity σ, and

$$\Pr\{\sigma\} = \prod_{k=1}^{N_\text{r}}\frac{1}{\Gamma_{\sigma_k}}\left[\sum_{m=1}^{k}\frac{1}{\Gamma_{\sigma_m}}\right]^{-1}. \tag{13}$$

By direct substitution, it can be verified that the instantaneous SNR's of the virtual paths are *conditionally* independent (conditioned upon the quantity σ) exponential random variables with *non*-identical means. Specifically, the conditional p.d.f. $f_{\boldsymbol{V}\big|_\sigma}(\{v_n\}_{n=1}^{N_\text{r}} \,\big|\, \sigma)$, is given by

$$f_{\boldsymbol{V}\big|_\sigma}(\{v_n\}_{n=1}^{N_\text{r}} \,\big|\, \sigma) = f_{V_1\big|_\sigma}(v_1 \,\big|\, \sigma) f_{V_2\big|_\sigma}(v_2 \,\big|\, \sigma)\ldots f_{V_{N_\text{r}}\big|_\sigma}(v_{N_\text{r}} \,\big|\, \sigma)\,, \tag{14}$$

where

$$f_{V_n\big|_\sigma}(v_n \,\big|\, \sigma) = \begin{cases} \frac{1}{\tilde{\Gamma}_n}e^{-\frac{v_n}{\tilde{\Gamma}_n}}, & 0 < v_n < \infty \\ 0, & \text{otherwise}\,, \end{cases} \tag{15}$$

with $\tilde{\Gamma}_n$ defined by

$$\tilde{\Gamma}_n \triangleq \left[\frac{1}{n}\sum_{m=1}^{n}\frac{1}{\Gamma_m}\right]\left[\frac{1}{n}\sum_{m=1}^{n}\frac{1}{\Gamma_{\sigma_m}}\right]^{-1}. \tag{16}$$

Note that $\tilde{\Gamma}_n$ is a function of σ. The characteristic function (c.f.) of V_n conditioned on σ is given by

$$\begin{aligned}\psi_{V_n|\sigma}(j\nu) &\triangleq \mathbb{E}\left\{e^{+j\nu V_n} \;\middle|\; \sigma\right\} \\ &= \frac{1}{1-j\nu\tilde{\Gamma}_n}\,.\end{aligned} \tag{17}$$

The instantaneous SNR of the combiner output can now be expressed in terms of the instantaneous SNR's of the virtual paths as

$$\gamma_{\text{SRake}} = \sum_{n=1}^{N_{\text{r}}} b_n V_n\,, \tag{18}$$

where the coefficients b_n's are given by

$$b_n\tilde{\Gamma}_n = \begin{cases}\left[\dfrac{1}{n}\displaystyle\sum_{m=1}^{n}\dfrac{1}{\Gamma_{\sigma_m}}\right]^{-1}, & n \le L \\ \left[\dfrac{1}{n}\displaystyle\sum_{m=1}^{n}\dfrac{1}{\Gamma_{\sigma_m}}\right]^{-1}\dfrac{L}{n}, & \text{otherwise}\,.\end{cases} \tag{19}$$

In terms of virtual path variables

$$P_{e,\text{SRake}} = \frac{1}{\pi}\int_0^{\Theta}\mathbb{E}_{\{V_n\}}\left\{e^{-\frac{\delta_{\text{MPSK}}}{\sin^2\theta}\sum_{n=1}^{N_{\text{r}}}b_nV_n}\right\}\,d\theta\,. \tag{20}$$

Using the chain rule of conditional expectations, (20) can be rewritten as:

$$\begin{aligned}P_{e,\text{SRake}} &= \mathbb{E}_{\sigma}\left\{\frac{1}{\pi}\int_0^{\Theta}\mathbb{E}_{V_n|\sigma}\left\{e^{-\frac{\delta_{\text{MPSK}}}{\sin^2\theta}\sum_{n=1}^{N_{\text{r}}}b_nV_n}\;\middle|\;\sigma\right\}\,d\theta\right\} \\ &= \mathbb{E}_{\sigma}\left\{P_{\text{SRake}}(e\mid\sigma)\right\}\,,\end{aligned} \tag{21}$$

where

$$\begin{aligned}P_{\text{SRake}}(e\mid\sigma) &\triangleq \frac{1}{\pi}\int_0^{\Theta}\mathbb{E}_{\left\{V_n|\sigma\right\}}\left\{e^{-\frac{\delta_{\text{MPSK}}}{\sin^2\theta}\sum_{n=1}^{N_{\text{r}}}b_nV_n}\;\middle|\;\sigma\right\}\,d\theta \\ &= \frac{1}{\pi}\int_0^{\Theta}\int_0^{\infty}\int_0^{\infty}\cdots\int_0^{\infty}e^{-\frac{c_{\text{MPSK}}}{2\sin^2\theta}\sum_{n=1}^{N_{\text{r}}}b_nV_n} \\ &\qquad\times\quad f_{\boldsymbol{V}|\sigma}(\{v_n\}_{n=1}^{N_{\text{r}}}\mid\sigma)\,dv_n\,d\theta\,.\end{aligned} \tag{22}$$

Exploiting the fact that the V_n's are conditionally independent, (22) becomes:

$$\begin{aligned} P_{\text{SRake}}(e \mid \sigma) &= \frac{1}{\pi}\int_0^{\Theta}\prod_{n=1}^{N_{\text{r}}}\mathbb{E}_{\left\{V_n\middle|\sigma\right\}}\left\{e^{-\frac{\delta_{\text{MPSK}}b_n}{\sin^2\theta}V_n}\;\middle|\;\sigma\right\}\,d\theta \\ &= \frac{1}{\pi}\int_0^{\Theta}\prod_{n=1}^{N_{\text{r}}}\psi_{V_n\middle|\sigma}\left(-\frac{\delta_{\text{MPSK}}b_n}{\sin^2\theta}\right)\,d\theta\,, \end{aligned} \tag{23}$$

where $\psi_{V_n\middle|\sigma}(\cdot)$ is given by (17). The utility of the virtual path technique is apparent by observing that the expectation operation in (9) no longer requires an N_{r}-fold nested integration.

Substituting (17) into (23) and together with (21), we arrive at the SEP for coherent detection of MPSK using the SRake receiver as

$$P_{e,\text{SRake}} = \sum_{\sigma\in\mathcal{S}_{N_{\text{r}}}}\Pr\{\sigma\}\;P_{\text{SRake}}(e\mid\sigma)\,, \tag{24}$$

where the conditional SEP, conditioned on σ, is given by

$$\begin{aligned} &P_{\text{SRake}}(e \mid \sigma) \\ &\quad= \frac{1}{\pi}\int_0^{\Theta}\prod_{n=1}^{L}\left[\frac{\sin^2\theta}{\delta_{\text{MPSK}}\left[\frac{1}{n}\sum_{m=1}^{n}\frac{1}{\Gamma_{\sigma_m}}\right]^{-1}+\sin^2\theta}\right] \\ &\qquad\times\prod_{n=L+1}^{N_{\text{r}}}\left[\frac{\sin^2\theta}{\delta_{\text{MPSK}}L\left[\sum_{m=1}^{n}\frac{1}{\Gamma_{\sigma_m}}\right]^{-1}+\sin^2\theta}\right]\,d\theta\,. \end{aligned} \tag{25}$$

Using the virtual branch technique and a similar procedure as for MPSK, the SEP for coherent detection of several two dimensional modulations can be derived. For example, the conditional SEP for coherent detection M-ary quadrature amplitude modulation (MQAM) with $M = 2^k$ for

even k, can be derived using techniques similar to [29] as

$$
\begin{aligned}
&P_{\text{SRake}}(e \mid \sigma) \\
&\quad = q\,\frac{1}{\pi}\int_0^{\pi/2}\prod_{n=1}^{L}\left[\frac{\sin^2\theta}{\delta_{\text{MQAM}}\left[\frac{1}{n}\sum_{m=1}^{n}\frac{1}{\Gamma_{\sigma_m}}\right]^{-1}+\sin^2\theta}\right] \\
&\qquad\qquad \times \prod_{n=L+1}^{N}\left[\frac{\sin^2\theta}{\delta_{\text{MQAM}}L\left[\sum_{m=1}^{n}\frac{1}{\Gamma_{\sigma_m}}\right]^{-1}+\sin^2\theta}\right] d\theta \\
&\quad -\frac{q^2}{4}\frac{1}{\pi}\int_0^{\pi/4}\prod_{n=1}^{L}\left[\frac{\sin^2\theta}{\delta_{\text{MQAM}}\left[\frac{1}{n}\sum_{m=1}^{n}\frac{1}{\Gamma_{\sigma_m}}\right]^{-1}+\sin^2\theta}\right] \\
&\qquad\qquad \times \prod_{n=L+1}^{N}\left[\frac{\sin^2\theta}{\delta_{\text{MQAM}}L\left[\sum_{m=1}^{n}\frac{1}{\Gamma_{\sigma_m}}\right]^{-1}+\sin^2\theta}\right] d\theta\,,
\end{aligned}
\tag{26}
$$

where $q = 4(1-\frac{1}{\sqrt{M}})$, and $\delta_{\text{MQAM}} = \frac{3}{2(M-1)}$.

Thus the derivation of the SEP for the SRake receiver involving the N_{r}-fold nested integrals in (10) essentially reduces to a single summation, each term requiring a single integral over θ with finite limits. The integrand is an N_{r}-fold product of simple expressions involving trigonometric functions. Note that the conditional independence of the virtual branch variables plays a key role in simplifying the derivation.

C. Special Case 1: The Single-Path Receiver

The SP receiver, also known as the selection diversity receiver, is the simplest form of diversity system whereby the received signal is selected from *one* of N_{r} diversity paths. The instantaneous

output SNR of the SP receiver is

$$\gamma_{\text{SP}} \triangleq \max_i \left\{\gamma_{[i]}\right\} = \gamma_{[1]}\,. \tag{27}$$

This is a special case of the SRake receiver with $L = 1$. Substituting $L = 1$ into (25) and (26), the conditional SEP $P_{\text{SP}}(e \mid \sigma)$ for coherent detection of MPSK and MQAM using the SP receiver becomes

$$\begin{aligned} &P_{\text{SP}}(e \mid \sigma) \\ &= \frac{1}{\pi}\int_0^{\Theta} \prod_{n=1}^{N_{\text{r}}} \left[\frac{\sin^2\theta}{\delta_{\text{MPSK}}\left[\sum_{m=1}^{n}\frac{1}{\Gamma_{\sigma_m}}\right]^{-1} + \sin^2\theta}\right] d\theta\,, \end{aligned} \tag{28}$$

and

$$\begin{aligned} &P_{\text{SP}}(e \mid \sigma) \\ &= q\,\frac{1}{\pi}\int_0^{\pi/2} \prod_{n=1}^{N_{\text{r}}} \left[\frac{\sin^2\theta}{\delta_{\text{MQAM}}\left[\sum_{m=1}^{n}\frac{1}{\Gamma_{\sigma_m}}\right]^{-1} + \sin^2\theta}\right] d\theta \\ &\quad -\frac{q^2}{4}\frac{1}{\pi}\int_0^{\pi/4} \prod_{n=1}^{N_{\text{r}}} \left[\frac{\sin^2\theta}{\delta_{\text{MQAM}}\left[\sum_{m=1}^{n}\frac{1}{\Gamma_{\sigma_m}}\right]^{-1} + \sin^2\theta}\right] d\theta\,, \end{aligned} \tag{29}$$

respectively.

D. Special Case 2: The All-Rake Receiver

For the ARake receiver, the signals from *all* Rake paths are weighted and combined to maximize the SNR at the combiner output. The instantaneous output SNR of the ARake receiver is given by

$$\gamma_{\text{ARake}} \triangleq \sum_{i=1}^{N_{\text{r}}} \gamma_i = \sum_{i=1}^{N_{\text{r}}} \gamma_{[i]}\,. \tag{30}$$

Note again that the result for the ARake receiver can be obtained from the SRake results given in (25) by setting $L = N_{\mathrm{r}}$, since the ARake is a special case of SRake with $L = N_{\mathrm{r}}$. Therefore, the conditional SEP $P_{\text{ARake}}(e \mid \sigma)$ for coherent detection of MPSK and MQAM using the ARake receiver becomes

$$P_{\text{ARake}}(e \mid \sigma) = \frac{1}{\pi} \int_0^{\Theta} \prod_{n=1}^{N_{\mathrm{r}}} \left[\frac{\sin^2\theta}{\delta_{\text{MPSK}} \left[\frac{1}{n} \sum_{m=1}^{n} \frac{1}{\Gamma_{\sigma_m}} \right]^{-1} + \sin^2\theta} \right] d\theta \,. \tag{31}$$

and

$$\begin{aligned} P_{\text{ARake}}(e \mid \sigma) &= q \, \frac{1}{\pi} \int_0^{\pi/2} \prod_{n=1}^{N_{\mathrm{r}}} \left[\frac{\sin^2\theta}{\delta_{\text{MQAM}} \left[\frac{1}{n} \sum_{m=1}^{n} \frac{1}{\Gamma_{\sigma_m}} \right]^{-1} + \sin^2\theta} \right] d\theta \\ &\quad - \frac{q^2}{4} \frac{1}{\pi} \int_0^{\pi/4} \prod_{n=1}^{N_{\mathrm{r}}} \left[\frac{\sin^2\theta}{\delta_{\text{MQAM}} \left[\frac{1}{n} \sum_{m=1}^{n} \frac{1}{\Gamma_{\sigma_m}} \right]^{-1} + \sin^2\theta} \right] d\theta \,, \end{aligned} \tag{32}$$

respectively.

III. Numerical results

In this section, we present numerical results obtained from the theoretical framework developed in Sec. II. The SEP is plotted as a function of the average SNR given as $\sum_{i=1}^{N} \Gamma_i$. This allows a comparison of Rake architectures with a different number of combined paths. Results based on the standardized channel models as well as on channel measurements will be presented.

A. Results based on channel models

The ITU-R [17] model was developed by the International Telecommunications Union. It specifies channel conditions for various operating environments encountered in third-generation wireless systems. This model has been adopted for the evaluation of third-generation cellular systems, such as 3GPP [9] and has also been used extensively for the simulation of other systems. It models the delay dispersion of the wireless propagation channel as a tapped-delay line, distinguishing between different radio environments. Table I gives the values of the tap delays and the associated mean powers of three different radio environments defined as Indoor-B, Pedestrian-B, and Vehicular-B.

We first analyze the performance of SRake receivers in a system with the bandwidth wide enough so that all taps are fading independently, i.e., with the bandwidth larger than or equal to 10 MHz for the profiles analyzed. Figure 1 gives the SEP for coherent detection of binary phase-shift keying (BPSK) using an SRake with different numbers of combined Rake fingers. The environment used in the figure is the Indoor-B profile, which has 6 independent fading multipath components. We see that most of the diversity gain can be obtained by utilizing three Rake fingers (about 3 dB at an SEP of 10^{-3}), while using three additional fingers gives less than 1 dB of incremental diversity gain.

A similar plot for the Pedestrian-B channel profile is shown in Fig. 2. It can be seen that the SEP in the Pedestrian-B environment is lower than in the Indoor-B environment. This is due to the fact that the differences among the average tap powers for the Pedestrian-B profile are smaller than for the Indoor-B profile, i.e., the Pedestrian-B profile is "more uniform" than the Indoor-B profile. Consequently, this results in a larger effective diversity gain.

Figure 3 shows the results for the Vehicular-B channel profile. The results are almost identical to the Indoor-B environment, which at first seems somewhat surprising in view of the different PDPs. The Vehicular-B PDP exhibits several widely separated paths with different strengths,

resulting in a root mean square (rms) delay spread of 4000 ns. On the other hand, the Indoor-B PDP exhibits a monotonic exponential decay with an rms delay spread of 100 ns. However, with negligible intersymbol interference and independent fading of the taps, only the relative tap power and the number of taps determine the performance.

Next, we investigate the influence of the spreading bandwidth on the performance of the SRake receiver. For this purpose, we consider the Indoor-B channel with various bandwidths. The bandwidths we consider are 10 MHz (independent fading), 5 MHz (W-CDMA), and 1.25 MHz (IS-95). Following the 3GPP recommendations, the power of a channel tap whose delay does not coincide with the center of a chip is distributed between the two chips it is closest to. Normalization was done so that the average received energy among all components is independent of the bandwidth.

Figure 4 shows the SEP as a function of the SNR for coherent detection of BPSK using an SRake with 1, 2, 3, and 6 fingers. We see that at low SNR's, there is negligible influence of the bandwidth on the SEP. At high SNR's, the larger bandwidth provides a higher degree of diversity, and thus gives considerably lower SEP. Intuitively, one would have expected that at low SNR's, a lower spreading bandwidth would result in a better performance since it allows the Rake fingers to capture more of the energy, but this effect is hardly noticeable in Fig. 4.

In order to further investigate the influence of the bandwidth on the SEP, we also consider a uniform PDP, i.e. equal mean power among the multipath components. The results are displayed in Fig. 5. Here, we observe that at SNR's below about 10 dB, a smaller spreading bandwidth results in better performance if the number of combined Rake fingers is small. The different behavior of exponential and rectangular PDP's can be explained intuitively: for an exponential decay, the first multipath component has a dominant influence, especially if the decay constant is large and the number of resolved multipath components is small (i.e. small spreading bandwidth). Consequently, the diversity gain is limited: if the first multipath component is in a deep fade,

the instantaneous Rake combiner output SNR is certainly low. For a larger bandwidth, the mean powers of the multipath components are more evenly distributed, so that fading of the first multipath component does not have such catastrophic consequences.

B. Results based on Channel Measurements

As a further check on our results, we present an example comparison with measured channel impulse responses. The measurements were performed in a macrocellular environment in Darmstadt, Germany with a channel sounder described in [30]. Measurements were made along a long route through the considered area. In order to make sure that only small-scale fading[4] (rather than shadowing) influences the fading statistics, we analyzed the "local regions of stationarity" (LRS) over which the statistics of the fading would stay wide-sense stationary. Details of this procedure can be found in [31]. We then chose one such LRS containing 273 measured channel impulse responses as our ensemble. The impulse responses were filtered with a raised-cosine filter with a bandwidth of 1.25 MHz (corresponding to the chip-rate of the IS-95 CDMA standard) and sampled at the same chip-rate. The resulting tap-delay line model formed the basis for our comparisons between theory and measurement.

For the "theory" results, we averaged the received power in each tap to arrive at the experimental PDP and generated the SEP curves according to (24)-(25) with $M = 2$. For the "measured" results, we identified for each measured impulse response the L strongest taps, added their powers, and inserted that power into the equation for the SEP in an AWGN channel [3] to obtain the conditional SEP (conditioned upon each of the measured impulse responses). We then averaged these conditional SEP's over our ensemble of 273 measured channel impulse responses to obtain the SEP in our measured channel.

Figure 6 shows a comparison of the SEP's computed by the two different methods. We see

[4]Small-scale fading is defined as fading caused by the constructive and destructive interference of several multipath components.

that at very high SNRs, the "measured" SEP is slightly lower than the theoretically computed one. This can be explained by the fact that the fading statistics of the received samples is not exactly Rayleigh, but that both very high and very low values of received power occur less frequently than in a true Rayleigh distribution as shown in Fig. 7. This leads on average to a lower SEP.

IV. Conclusions

We derived the symbol error probability (SEP) of the SRake receiver in a frequency selective multipath fading environment with a nonuniform PDP. We analyzed this system using a "virtual path" technique, which resulted in a simple derivation and formulas for any L and N_{r}. The key idea was to transform the dependent ordered paths into a new set of conditionally independent virtual paths, and express the SRake output SNR as a linear combination of the conditionally independent virtual paths. Comparisons with simulations based on synthetic channel models, as well as measurements, confirmed our computations. We found that the shape of the PDP has a large influence on the possible diversity gain. For a fixed number of Rake fingers, increasing the spreading bandwidth is advantageous at large SNR but detrimental at low SNR. The transition between those two cases occurs at a higher SNR for uniform PDPs and at a lower SNR for exponential PDPs.

Acknowledgments

The authors wish to thank L. A. Shepp, and C. L. Mallows for helpful discussions. The financial support of the Austrian Ministry of Science and the TU Wien for part of the work of Andreas F. Molisch is gratefully acknowledged.

REFERENCES

[1] R. L. Pickholtz, D. L. Schilling, and L. B. Milstein, "Theory of spread-spectrum communications – A tutorial," *IEEE Trans. Commun.*, vol. COM-30, no. 5, pp. 855–884, May 1982.

[2] M. K. Simon, J. K. Omura, R. A. Scholtz, and B. K. Levitt, *Spread Spectrum Communications Handbook*, electronic ed. New York, NY, 10020: McGraw-Hill, Inc., 2001.

[3] J. G. Proakis, *Digital Communications*, 4th ed. New York, NY, 10020: McGraw-Hill, Inc., 2001.

[4] A. F. Molisch, Ed., *Wideband Wireless Digital Communications*. Upper Saddle River, New Jersey 07458: Prentice Hall Publishers, 2001.

[5] F. Adachi, M. Sawahashi, and H. Suda, "Wideband DS-CDMA for next-generation mobile communications systems," *IEEE Commun. Mag.*, vol. 36, no. 9, pp. 56–69, Sept. 1998.

[6] N. Benvenuto, E. Costa, and E. Obetti, "Performance comparison of chip matched filter and RAKE receiver for WCDMA systems," in *Proc. IEEE Global Telecomm. Conf.*, vol. 5, Nov. 2001, pp. 3060–3064, san Antonio, TX.

[7] T. Ojanpera and R. Prasad, "An overview of air interface multiple access for IMT-2000/UMTS," *IEEE Commun. Mag.*, vol. 36, no. 9, pp. 82–95, Sept. 1998.

[8] H. Holma and A. Toskala, *WCDMA for UMTS: Radio Access for Third Generation Mobile Communications*, revised ed. New York, NY 10158-0012: John Wiley & Sons, Inc., 2002.

[9] [Online]. Available: http://www.3gpp.org

[10] [Online]. Available: http://www.3gpp2.org

[11] M. Z. Win and R. A. Scholtz, "On the energy capture of ultra -wide bandwidth signals in dense multipath environments," *IEEE Commun. Lett.*, vol. 2, no. 9, pp. 245–247, Sept. 1998.

[12] T. Eng, N. Kong, and L. B. Milstein, "Comparison of diversity combining techniques for Rayleigh-fading channels," *IEEE Trans. Commun.*, vol. 44, no. 9, pp. 1117–1129, Sept. 1996.

[13] K. J. Kim, S. Y. Kwon, E. K. Hong, and K. C. Whang, "Comments on "comparison of diversity combining techniques for Rayleigh-fading channels"," *IEEE Trans. Commun.*, vol. 46, no. 9, pp. 1109–1110, Sept. 1998.

[14] L. M. Jalloul and J. M. Holtzman, "Multipath fading effect on wide-band DS/CDMA signals: Analysis, simulation, and measurements," *IEEE Trans. on Veh. Technol.*, vol. 43, no. 3, pp. 801–807, Aug. 1994.

[15] N. Kong and L. B. Milstein, "Combined average SNR of a generalized diversity selection combining scheme," in *Proc. IEEE Int. Conf. on Commun.*, vol. 3, June 1998, pp. 1556–1560, atlanta, GA.

[16] M. Z. Win, G. Chrisikos, and N. R. Sollenberger, "Performance of Rake reception in dense multipath channels: Implications of spreading bandwidth and selection diversity order," *IEEE J. Select. Areas Commun.*, vol. 18, no. 8, pp. 1516–1525, Aug. 2000.

[17] International Telecommunications Union, "Guidelines for evaluation of radio transmission technologies for IMT-2000," Recommendation ITU-R M.1225, 1997.

[18] E. Failli, Ed., *Digital land mobile radio. Final report of COST 207*. Luxemburg: Commission of the European Union, 1989.

[19] M. Z. Win, G. Chrisikos, A. F. Molisch, and N. R. Sollenberger, "Selective Rake diversity in multipath fading with arbitrary power delay profile," in *Proc. IEEE Global Telecomm. Conf.*, vol. 2, San Francisco, CA, Dec. 2000, pp. 960–964.

[20] M.-S. Alouini and M. K. Simon, "A compact performance analysis of generalized selection combining with independent but nonidentically distributed Rayleigh fading paths," *IEEE Trans. Commun.*, vol. 50, no. 9, pp. 1409–1412, Sept. 2002.

[21] J. E. Mazo, "Exact matched filter bounds for two-beam Rayleigh fading," *IEEE Trans. Commun.*, vol. 39, no. 7, pp. 1027–1030, July 1991.

[22] M. V. Clark, L. J. Greenstein, W. K. Kennedy, and M. Shafi, "Matched filter performance bounds for diversity combining receivers in digital mobile radio," *IEEE Trans. on Veh. Technol.*, vol. 41, no. 4, pp. 356–362, Nov. 1992.

[23] N. J. Baas and D. P. Taylor, "Matched filter bounds for wireless communication over Rayleigh fading dispersive channels," *IEEE Trans. Commun.*, vol. 49, no. 9, pp. 1525–1528, Sept. 2001.

[24] E. Chiavaccini and G. M. Vitetta, "Error performance of matched and partially matched one-shot detectors for doubly selective Rayleigh fading channels," *IEEE Trans. Commun.*, vol. 49, no. 10, pp. 1738–1747, Oct. 2001.

[25] C. Tellambura, A. J. Mueller, and V. K. Bhargava, "Analysis of M-ary phase-shift keying with diversity reception for land-mobile satellite channels," *IEEE Trans. on Veh. Technol.*, vol. 46, no. 4, pp. 910–922, Nov. 1997.

[26] M. K. Simon and D. Divsalar, "Some new twists to problems involving the Gaussian probability integral," *IEEE Trans. Commun.*, vol. 46, no. 2, pp. 200–210, Feb. 1998.

[27] M.-S. Alouini and A. Goldsmith, "A unified approach for calculating error rates of linearly modulated signals over generalized fading channels," *IEEE Trans. Commun.*, vol. 47, no. 9, pp. 1324–1334, Sept. 1999.

[28] M. K. Simon and M.-S. Alouini, *Digital Communication over Fading Channels: A Unified Approach to Performance Analysis*, 1st ed. New York, NY, 10158: John Wiley & Sons, Inc., 2000.

[29] M. Z. Win and J. H. Winters, "Virtual branch analysis of symbol error probability for hybrid selection/maximal-ratio combining in Rayleigh fading," *IEEE Trans. Commun.*, vol. 49, no. 11, pp. 1926–1934, Nov. 2001.

[30] K. Schwarz, U. Martin, and H. Schüsler, "Devices for propagation measurement in mobile radio channels," in *Proc. 4th IEEE Int. Symp. on Personal, Indoor and Mobile Radio Communications*, Sept. 1993, pp. 387–391, yokohama, JAPAN.

[31] M. Steinbauer, "The radio propagation channel - a nondirectional, directional, and double-directional point of view," Ph.D. dissertation, Technical University of Vienna, Vienna, AUSTRIA, May 2002.

TABLE I

PARAMETERS FOR INDOOR-B, PEDESTRIAN-B, AND VEHICULAR-B RADIO ENVIRONMENTS

Tap No.	Delay [μs]	Power [dB]	Fractional Power
INDOOR B			
1	0	-2.4	0.578
2	0.1	-6.0	0.253
3	0.2	-9.6	0.110
4	0.3	-13.2	0.048
5	0.5	-20.4	0.009
6	0.7	-27.6	0.002
PEDESTRIAN B			
1	0	-3.9	0.406
2	0.2	-4.8	0.330
3	0.8	-8.8	0.131
4	1.2	-11.9	0.064
5	2.3	-11.7	0.067
6	3.7	-27.8	0.002
VEHICULAR B			
1	0	-4.9	0.323
2	0.3	-2.4	0.574
3	8.9	-15.2	0.030
4	12.9	-12.4	0.057
5	17.1	-27.6	0.002
6	20.2	-18.4	0.014

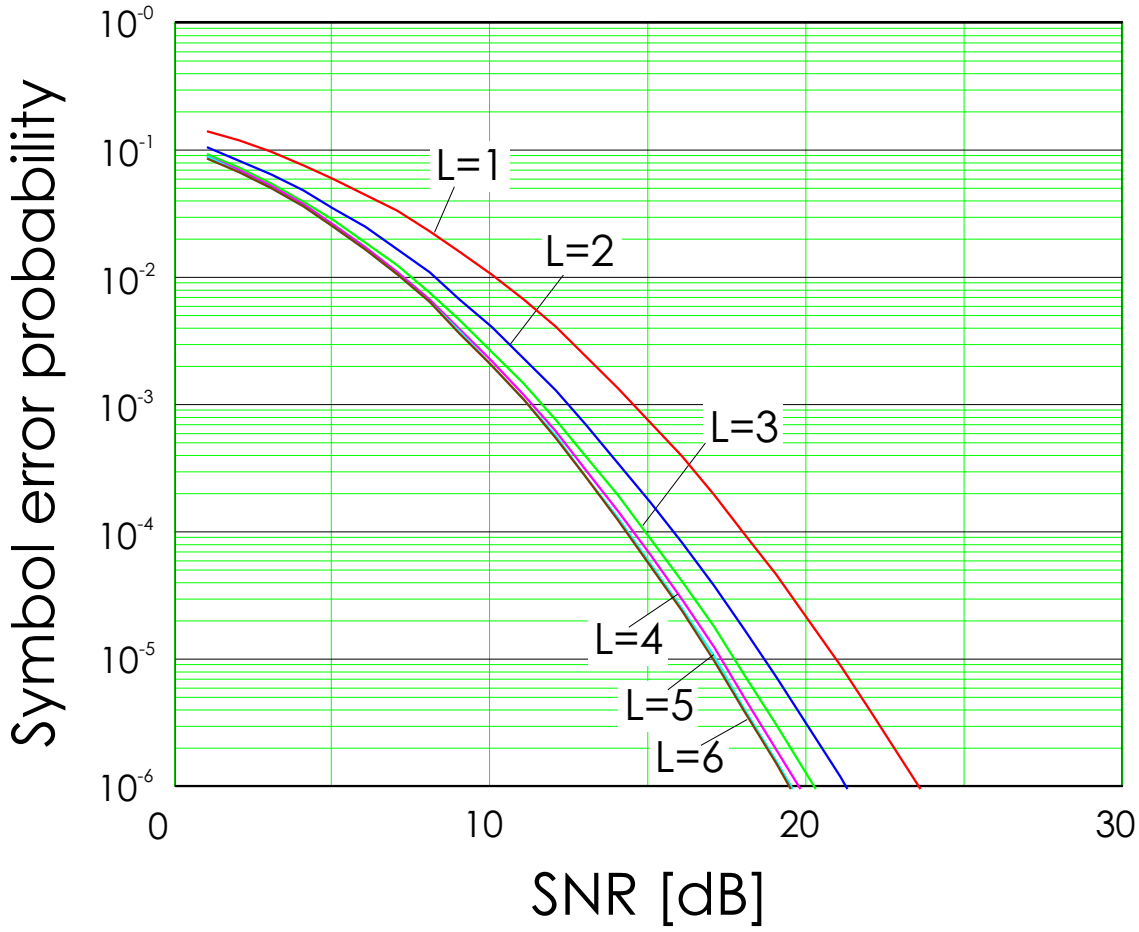

Fig. 1. Symbol error probability as a function of the average SNR using an SRake receiver with L fingers in a Indoor-B environment.

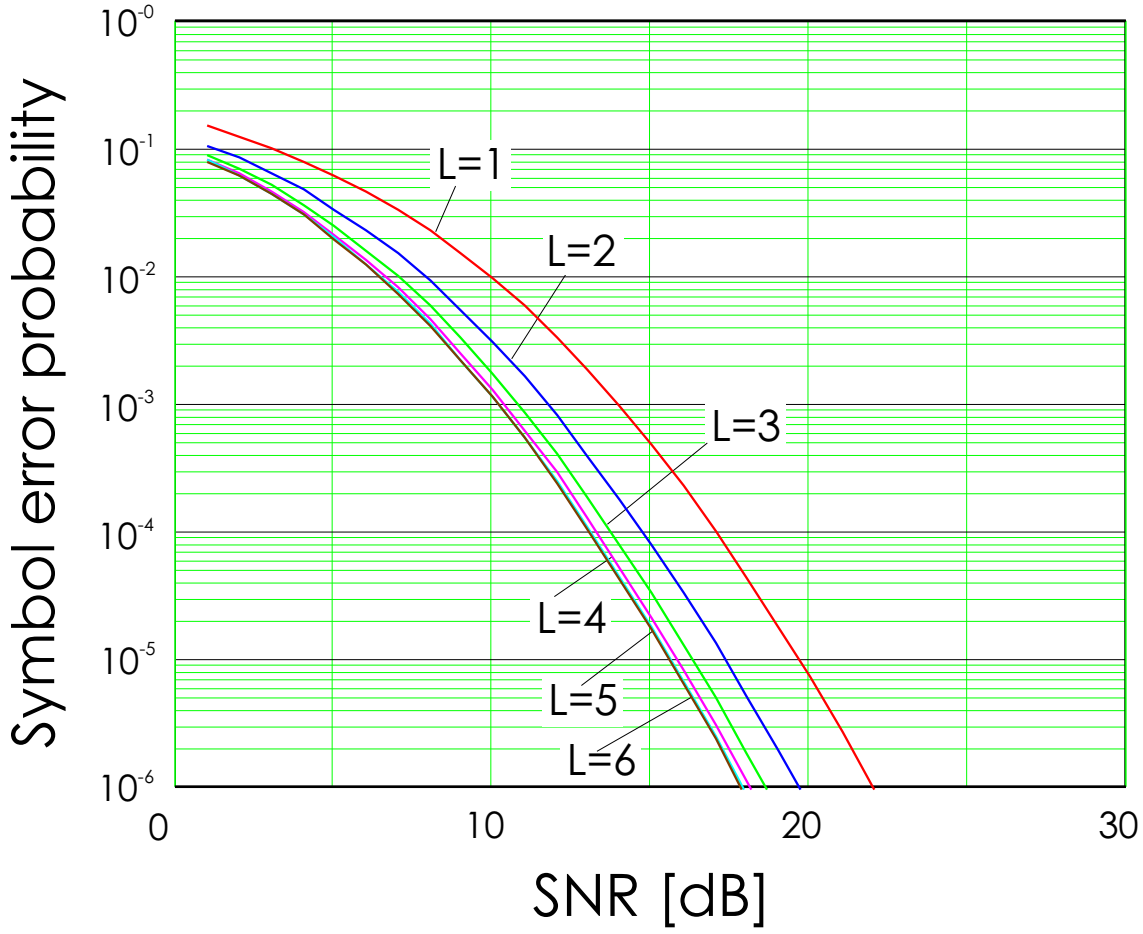

Fig. 2. Symbol error probability as a function of the average SNR using an SRake receiver with L fingers in a Pedestrian-B environment.

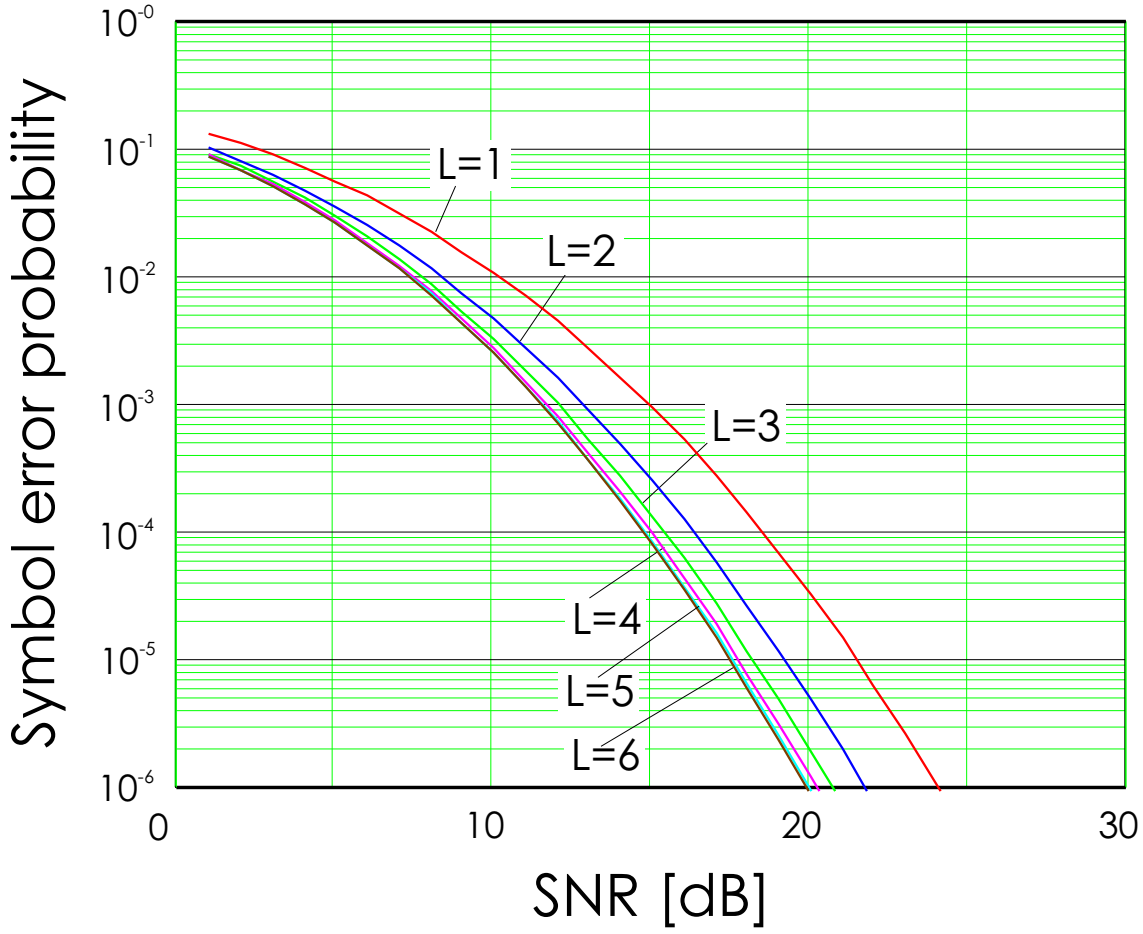

Fig. 3. Symbol error probability as a function of the average SNR using an SRake receiver with L fingers in a Vehicular-B environment.

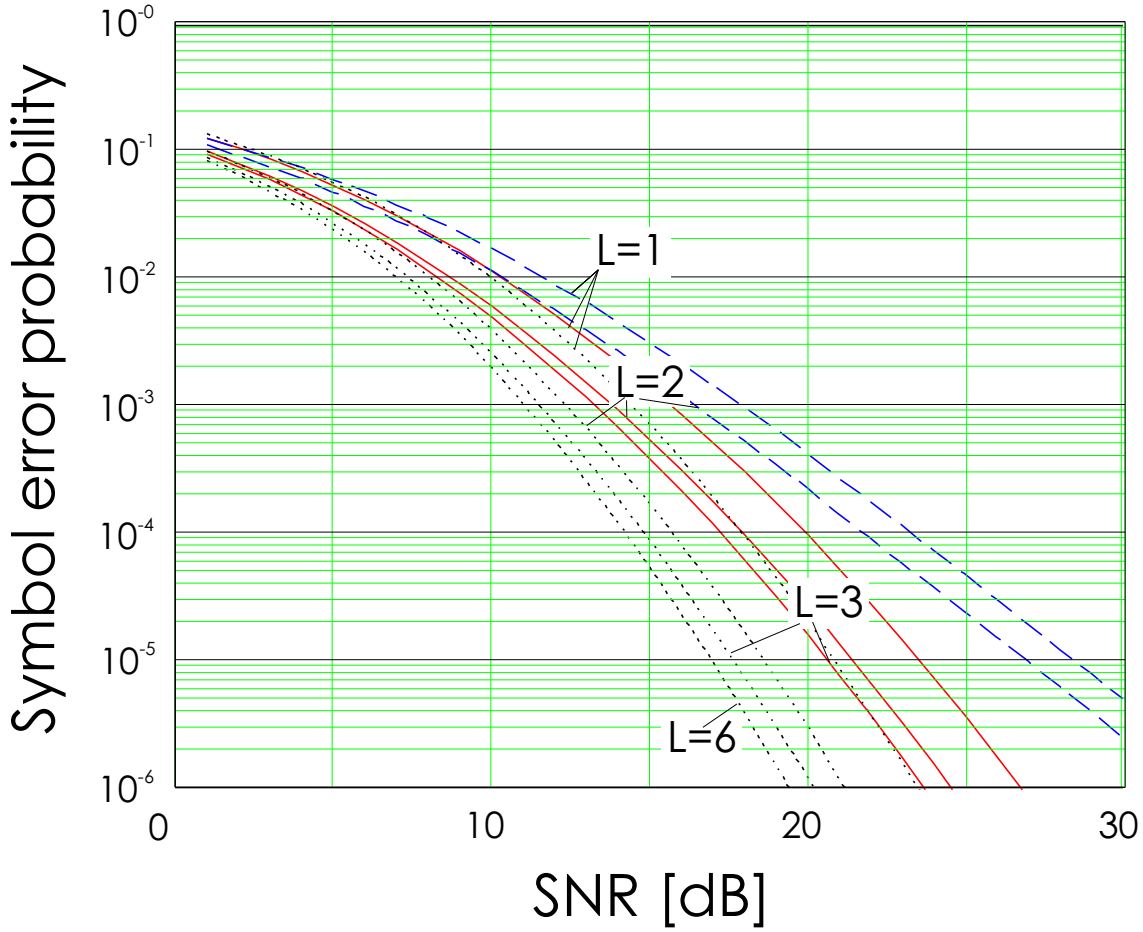

Fig. 4. Symbol error probability using an SRake receiver with L fingers in a channel having Indoor-B power delay profile. The bandwidth is 1.25 MHz (dashed lines), 5 MHz (solid lines), or 10 MHz (dotted lines). The total number of resolved multipath components is 2, 5, or 6 respectively.

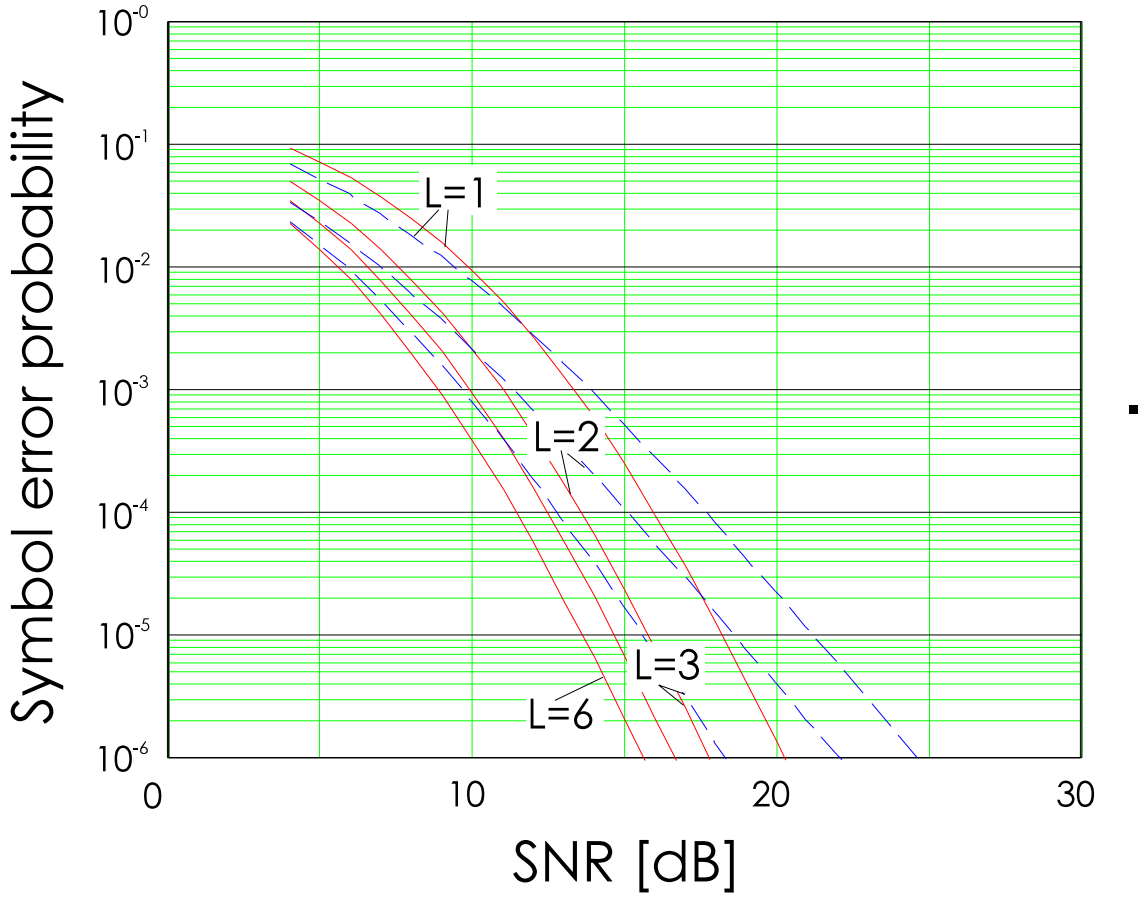

Fig. 5. Symbol error probability using an SRake receiver with L fingers in a channel having uniform power delay profile. The multipath components are spaced regularly at $i \times 100$ ns, with $i = 0, ...5$. The system bandwidth is 10 MHz (solid lines) and 5 MHz (dashed lines). No power splitting was employed for non-centered taps.

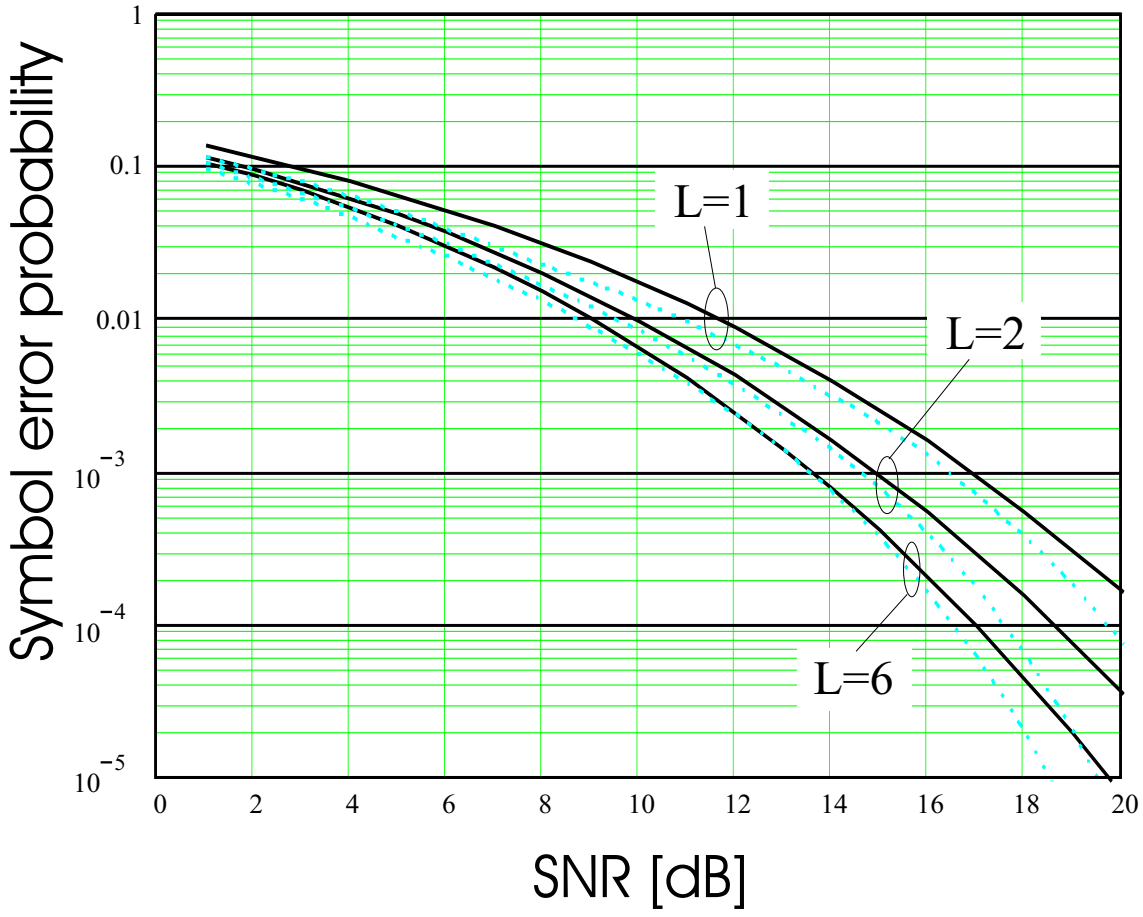

Fig. 6. Symbol error probability for the considered LRS: theory (solid) and measured (dotted) for $L = 1, 2$, and 6 fingers. The theory results use average powers of the multipath components in Eq. (25) to compute the SEP. The measured results compute the instantaneously best multipath components and use their power in Eq. (8).

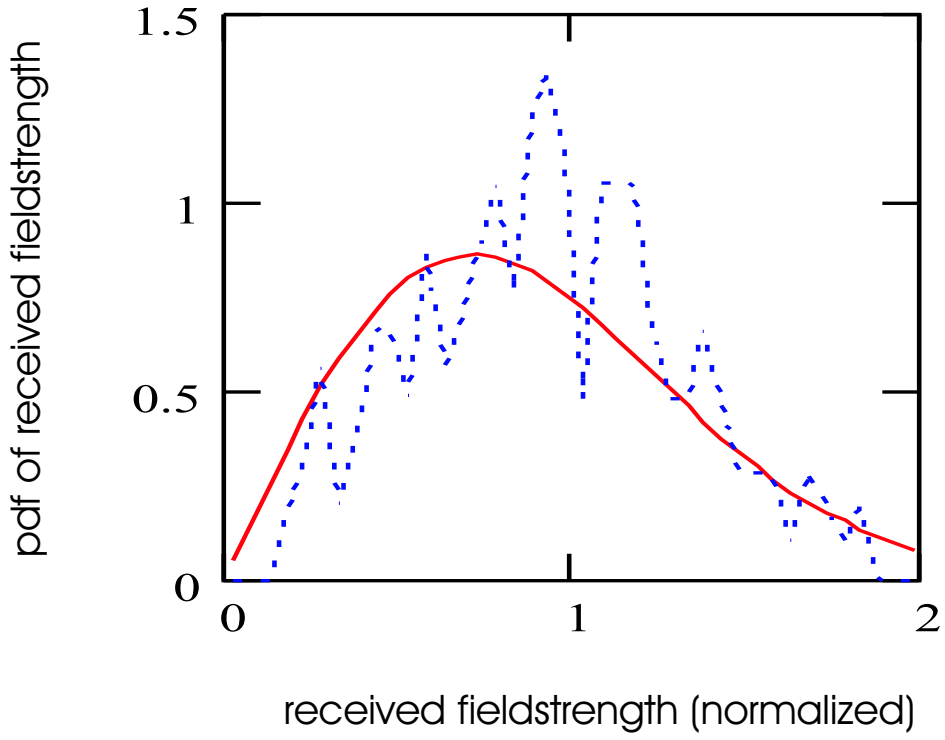

Fig. 7. Probability density function of the field strength as measured in the considered LRS (dotted) and for a Rayleigh fading channel (solid).